Structural Transition During Fibrillogenesis of Amyloid β Peptide

2017

George Sidrak
University of Central Florida

STRUCTURAL TRANSITION DURING FIBRILLOGENESIS OF AMYLOID β PEPTIDE

by

GEORGE SIDRAK

A thesis submitted in partial fulfillment of the requirements
for the Honors in the Major Program in Biomedical Sciences
in the Burnett School of Biomedical Sciences
and in The Burnett Honors College
at the University of Central Florida
Orlando, Florida

Spring Term, 2017

Thesis Chair: Dr. Suren Tatulian

ABSTRACT

Alzheimer's Disease (AD) is a neurodegenerative disease marked by progressive neuronal cell death, leading to dementia. AD is the most common disease that results in dementia and largely affects the elderly, with five million people in the United States diagnosed with the disease as of 2015 and approximately 35 million people worldwide. Diseases resulting in dementia cost the US healthcare system an estimated $172 billion in 2010 and that cost is expected to increase as the population ages and as diagnostic techniques improve so that more people are treated (Holtzman, 2011). The disease was first reported by psychiatrist Alois Alzheimer at the onset of the 20th century, when one of his patients "suffered memory loss, disorientation, hallucinations and delusions and died at the age of 55," then was found to have severe brain atrophy post-mortem (Cipriani, Dolciotti, Picchi, & Bonuccelli, 2011). There are palliative treatments available that marginally slow disease progression but there is currently no cure for the disease (Awasthi, Singh, Pandey, & Dwivedi, 2016). More research is needed to develop effective therapeutic strategies to combat the disease. Currently, AD cytotoxicity is believed to be caused by increased amyloid β (Aβ) peptide plaque deposition in the brain, as described by the amyloid cascade hypothesis (Barage & Sonawane, 2015). The current understanding is that oligomers of Aβ peptide lead to neuronal death through multiple mechanisms, most notably hyper-phosphorylation of the tau protein. Having a better understanding of the structural changes in the fibrillization process of Aβ will provide a broader insight into mechanisms of cell death and open new possibilities for pharmacological treatments, which is what this research intends to provide.

ACKNOWLEDGEMENTS

I would like to thank Dr. Greg Goldblatt, my mentor who first taught me how to navigate in a research lab.

Dr. Bo Chen and Dr. Ken Teter, the rest of my thesis committee, for bearing with me through many proposal and thesis revisions throughout the process of thesis writing.

And Dr. Suren Tatulian, my thesis chair, who introduced me to the world of research and the study of amyloid beta fibrillogenesis.

TABLE OF CONTENTS

LIST OF FIGURES

LITERATURE REVIEW

Amyloidosis

Amyloidosis refers to a class of degenerative diseases, caused by protein aggregation. The amyloidosis process forms fibrils with characteristic cross β sheet structure (Ankarcrona, et al., 2016). The diseases vary in whether protein accumulation is localized to an organ (ex. AD or Type 2 Diabetes Mellitus) or if protein accumulation is systemic (ex. Transthyretin amyloidosis). Clinically, only the symptoms of this group of diseases are able to be treated, given the complexity and lack of understanding at the molecular level of disease process.

Types of Alzheimer's Disease

Alzheimer's Disease is classified into two subtypes: Sporadic Alzheimer's Disease (SAD) and Familial Alzheimer's Disease (FAD), with FAD being further divided into early onset and late onset. SAD makes up about 75% of AD cases, while FAD constitutes the other 25%. Out of FAD, about 95% is late onset and 5% is early onset (Bird, 2015). SAD is typically the AD form that is encountered with increasing patient age, while FAD is genetically inherited through familial lines. Despite having different terms of onset and origins, all of the AD classifications have the same source of cytotoxicity and are histologically indistinguishable (Takei, Kosarac, & Powell, 2009). AD neurons, especially in the hippocampus, are marked by neurofibrillary tangles (NFT's), granulovacuolar degeneration (GVD), and senile plaques (SP's) of Aβ (Takei, Kosarac, & Powell, 2009). Currently, treatment of AD uses donepezil, galantamine, rivastigmine, and memantine, which have the ability to slow disease progression but do no target underlying amyloid fibrillogenesis. To date, there have been experimental AD

treatments that slowed Aβ fibrillogenesis in vitro, but none have successfully passed FDA stage III clinical trials (Herrmann, Chau, Kircanski, & Lanctot, 2011; Ehret & Chamberlin, 2015; Ankarcrona, et al., 2016).

Amyloid Beta Fibrillogenesis

The amyloid precursor protein (APP) is a multidomain transmembrane protein commonly present in neuronal synapses as well as neuromuscular synapses. In the CNS, the APP has been shown to have multiple functions, including cell-cell adhesion, formation of new synapses, and signal transduction. Secreted APP (sAPP) has also been implicated in neuron growth (Gralle & Ferreira, 2007; Klevanski, et al., 2015). The APP is also involved in the development of neuromuscular synapses (Klevanski, et al., 2015). There are two studied APP metabolic pathways. One of the APP metabolic pathways leads to Aβ deposition and the clinical symptoms known as AD, and is termed the amyloidogenic pathway. It starts with the APP being sequentially cleaved by β-secretase then γ-secretase, forming sAPP, an amyloid intracellular domain fragment (AICD), and Aβ (Mohamed, Shakeri, & Rao, 2016; Agostinho, Pliassova, C.R., & R.A., 2015) (**Figure 1**). Due to the poor specificity of γ-secretase, Aβ can be either 40, 42, or 49 residues long, with 40- and 42-amino acid peptides ($A\beta_{1\text{-}40}$ and $A\beta_{1\text{-}42}$) being the most common (Beel & Sanders, 2008; O'Brien & PC, 2011). The non-amyloidogenic pathway starts with the APP being cleaved with α-secretase then γ-secretase, and does not result in Aβ production.

Aβ monomers are hydrophobic, which results in peptide aggregation in aqueous environments of intracellular and extracellular spaces, unless broken down through other metabolic pathways. In the AD brain, Aβ often undergoes post-secretase cleavage modifications

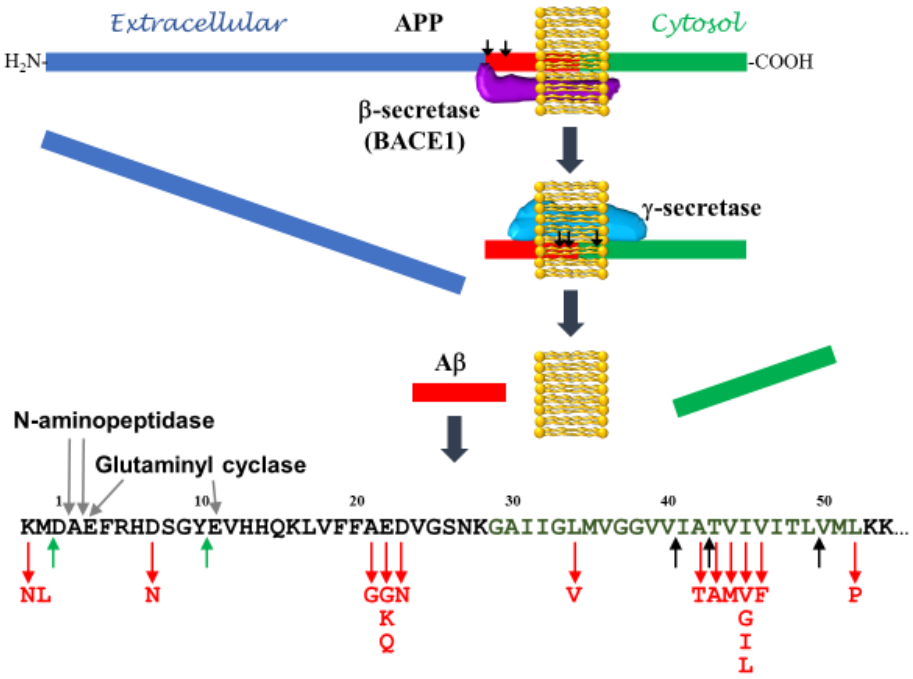

Figure 1

Cartoon showing APP's processing by β- and γ-secretases, Aβ sequence, modifications, and disease-related mutations. The extracellular and cytosolic stretches of APP are shown as blue and green bars, and the sequence corresponding to Aβ is shown in red. The cell plasma membrane is shown as a yellow lipid bilayer. The sequential action of β- and γ-secretases is shown in the upper part, where the respective cleavage sites are schematically shown by small downward arrows. The sequence comprising Aβ is shown at the lower part, where the transmembrane domain (residues 29-52 of Ab or 700-723 of APP) is shown in green. Cleavage sites for β- and γ-secretases are shown by green and black upward arrows, respectively. Sites for N-aminopeptidase and glutaminyl cyclase are shown by gray arrows. Genetic (familial) mutations related to AD are shown by red downward arrows.

like amino or carboxy terminal trimming – most notably amino truncated peptides, which can comprise up to half of the total Aβ load. Complex oligomers of both the full-length peptide and N-truncated peptides have been shown to be the main cytotoxic entity in AD, with increased neurotoxicity and increased aggregation (Bayer & Wirths, 2014). If not otherwise broken apart by proteolytic enzymes or cleared by the immune system, these oligomers continue to aggregate into distinct protofibrils and then to fibrils, which are the hallmark "amyloid plaques" that are found in post-mortem AD brains (Takei, Kosarac, & Powell, 2009).

Genetics of AD

During the 1970's in a groundbreaking study, AD was found to be strongly correlated with patients who also had Down Syndrome or trisomy 21, leading to the hypothesis that human chromosome 21 was involved in AD (Hetson, 1977). Later on, it was found that chromosome 21 contains the *APP* gene, and that certain single nucleotide polymorphisms on that loci were correlated with FAD (Miller, Currie, Iqbal, Potempska, & Styles, 1989; Lin, Wang, Wang, Liao, & Cheng, 2014). Aβ is generated from APP after cleavage by γ-secretase, which is coded by presenilin 1 and 2 (PSEN 1 and 2) on chromosome 14. SNPs here can cause upregulation of the enzyme and therefore an earlier onset of FAD (Jayne, et al., 2016).

Normally, apolipoproteins in the interstitial space of the brain are responsible for clearing the extracellular matrix (ECM) of debris, like amyloid fragments and oligomers. However, isoforms of the protein coded by the APOE gene on chromosome 19 are known to be more contributory to AD pathogenesis, or more able to guard against AD. The three most common

isoforms of apolipoprotein are ε2, ε3, and ε4. ε2 guards against AD, ε3 is the most common in the general population, and ε4 contributes to AD pathogenesis (Lim, et al., 2015).

Tau Protein

The tau protein supports intracellular microtubule structure in healthy central nervous system neurons. As part of neurodegenerative diseases such as AD and Parkinson's Disease, tau proteins become hyperphosphorylated with exponential kinetics. This disrupts their interactions with the neuron's cytoskeleton, causing them to lose their support function and form disruptive neurofibrillary tangles (NFT's) (Goedert, 2015). NFT's are intracellular aggregates of tau protein. This process can be triggered by Aβ being internalized into neurons, as well as through other mechanisms. The details of these mechanisms remain to be elucidated, but current research suggests that these occur through a prion-like action (Goedert, 2015).

Pyroglutamylated Aβ

Normally, glutaminyl-cyclase functions in the hypothalamus to activate thyrotropin-releasing hormone and gonadotropin-releasing hormone through pyroglutamylation. However, this enzyme is not specific to just these hormones and is known to act on other peptides also in the brain (Schilling, et al., 2011). Pyroglutamylated Aβ forms when N-truncated Aβ is further processed by glutaminyl-cyclase, most commonly at the residue 3 glutamate but also at the residue 11 glutamate (Mandler, et al., 2014). This amyloid species is clinically relevant because its presence, when in combination with the full length peptide, is correlated with the severity of AD (Mandler, et al., 2014). In vitro, combinations of $A\beta_{1\text{-}42}$ and $A\beta_{pE3\text{-}42}$ have been shown to form more stable oligomers than either peptide on its own, and that these combinations have a

lower propensity to form fibrils (Goldblatt, Matos, Gornto, & Tatulian, 2015). It is believed that this stabilization of oligomers is what causes the presence of pyroglutamylated Aβ to be correlated with more adverse outcomes in AD.

$A\beta_{1-40}$ Compared to $A\beta_{1-42}$ Structure

The last two amino acids that are present in $A\beta_{1-42}$ but not in $A\beta_{1-40}$, an isoleucine and an alanine, seem to have a significant effect on fibril structure. Compared to fibrils seeded by $A\beta_{1-40}$, fibrils seeded by $A\beta_{1-42}$ show greater stability (Paravastu, Leapman, Yau, & Tycko, 2008; Tycko, 2016). The hydrophobicity of those two amino acids is likely what is having this stabilizing effect on fibrils. However, there is very limited research on precise oligomeric structure and transitional differences between the two species. Previously, our lab has studied the structural transition in the 42-length Aβ, and found that a combination of pyroglutamylated and non-pyroglutamylated leads to inhibition of fibrillogenesis (Goldblatt, Matos, Gornto, & Tatulian, 2015). However, the structural transition of 40-length oligomers has not yet been studied. This study intends to explore the structural transition of the 40-length Aβ, and especially the impact of pyroglutamylation at residue 3 will have on this process.

OBJECTIVE

The goal of this study is to observe the structural changes that occur during $A\beta_{1\text{-}40}$ and $A\beta_{pE3\text{-}40}$ fibrillogenesis when separated and in combination, in order to gain a better understanding of the molecular basis of AD pathophysiology. Although $A\beta_{1\text{-}40}$ and $A\beta_{pE3\text{-}40}$ have been studied separately, there is little literature on their structure in combination, which is more akin to AD pathophysiology. Studies on $A\beta_{1\text{-}42}$ and $A\beta_{pE3\text{-}42}$ have shown that pyroglutamylated Aβ can stabilize oligomer structure, meaning it would be important to see how this modification affects the 40-length peptide, which is actually more abundant in the CNS. Fourier Transform Infrared (FTIR) spectroscopy is the optimal technique to do this, since if one peptide is labeled with ^{13}C, both structures can be discerned even when the two peptides are in combination. Better understanding of these structural changes opens a venue for novel AD immunodiagnostic and therapeutic techniques.

METHODOLOGY

Circular Dichroism

Circular Dichroism (CD) is a spectroscopic technique based on electron transitions commonly used to study protein secondary structure. The difference in absorption of right-hand and left-hand circularly polarized ultraviolet light yields CD spectra that indicate a protein's secondary structure (Miles & Wallace, 2016). In this study, CD was used to establish a baseline secondary structure of the peptides while dissolved in hexafluoroisopropanol (HFIP) to complement the FTIR data.

Fourier Transform Infrared Spectroscopy

FTIR spectroscopy is a powerful technique that uses a broad range of infrared light to obtain high resolution data that is made into a spectrum with Fourier Transform. It is especially useful for the study of amyloidosis, in which protein structure is transitioning making the process difficult to study with NMR or X-ray crystallography. Protein secondary structure is shown in two regions, amide I (1700-1600cm^{-1}) and amide II (1600-1500cm^{-1}). For this experiment, ^{13}C isotopes have been incorporated into the backbone of $A\beta_{1\text{-}40}$ peptide, which results in dissection of $A\beta_{1\text{-}40}$ and $A\beta_{pE3\text{-}40}$ FTIR signals due to a spectral shift of the ^{13}C-labeled peptide and thereby allows determination of structural changes in both peptides when they are combined in the same sample. The ^{13}C heavier carbon causes a 40-44cm^{-1} spectral downshift of the infrared amide I absorbance band that reflects the peptide backbone structure (i.e., α-helix and β-sheet), meaning the structure of the ^{13}C-labeled full length peptide will be shown at a lower frequency than the unlabeled pyroglutamylated peptide.

Procedure

This study explores the structural transitions of uniformly ^{13}C labeled $A\beta_{1\text{-}40}$ and unlabeled $A\beta_{pE3\text{-}40}$ peptides separately, and combined in a 1:1 molar ratio. The structural changes will be observed with FTIR, using a Vector-22 FTIR spectrometer (Bruker Optics, Billerica, MA, USA). Lyophilized peptides bought from rPeptide are first dissolved in HFIP to break up any pre-formed protein aggregates and CD measurements are taken. Due to its polarity and preference of forming hydrogen bonds, HFIP prevents the formation of inter- and intramolecular hydrogen bonding in Aβ that normally support the aggregation of monomers. This effect also causes Aβ to take a α-helix conformation, which makes this step more relevant because the Aβ domain of APP is also in a α-helix conformation before being proteolytically cleaved.

The solution is placed on a CaF_2 window, and desiccated to remove the HFIP. The FTIR spectrum of the dry peptide sample is measured. A pH 7.2 (pD 6.8) D_2O-based buffer containing 50 mM NaCl and 50 mM Na,K-phosphate is then added to the sample, so that it reaches a 50 μM final concentration. D_2O is used instead of H_2O because normal H_2O absorbs strongly in the amide I region. This buffer is meant to mimic ionic conditions present in the brain. Cerebrospinal fluid normally has a pH range of 7.28-7.32, a sodium concentration of 135-150mM, a potassium concentration of 2.7-3.9mM, and a chloride concentration of 116-127mM (Sofronescu, 2015). 300 scans of FTIR are taken of the dry peptide(s), once aqueous buffer is added, then at 10 minute, 30 minute, 60 minute and 120 minute marks after the addition of buffer.

CIRCULAR DICHROISM DATA

^{13}C-Labeled Aβ$_{1-40}$, Aβ$_{pE3-40}$

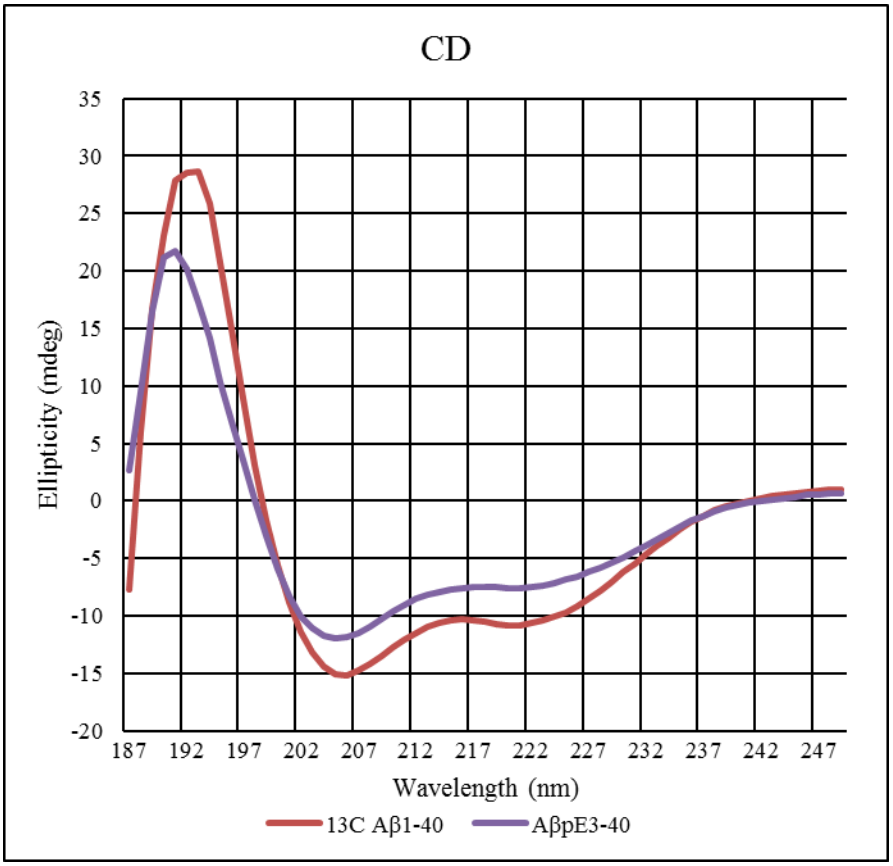

Figure 2

Circular dichroism measurements of the two peptides in HFIP were taken to determine the starting structures of the peptides. Both the ^{13}C-labeled Aβ$_{1-40}$ and Aβ$_{pE3-40}$ peptides displayed a positive maximum signal around 190-192 nm, and two negative minima at 205 nm and 225 nm, indicating that both peptides are in α-helix conformation while dissolved in HFIP.

FTIR DATA

^{13}C-Labeled Aβ$_{1-40}$

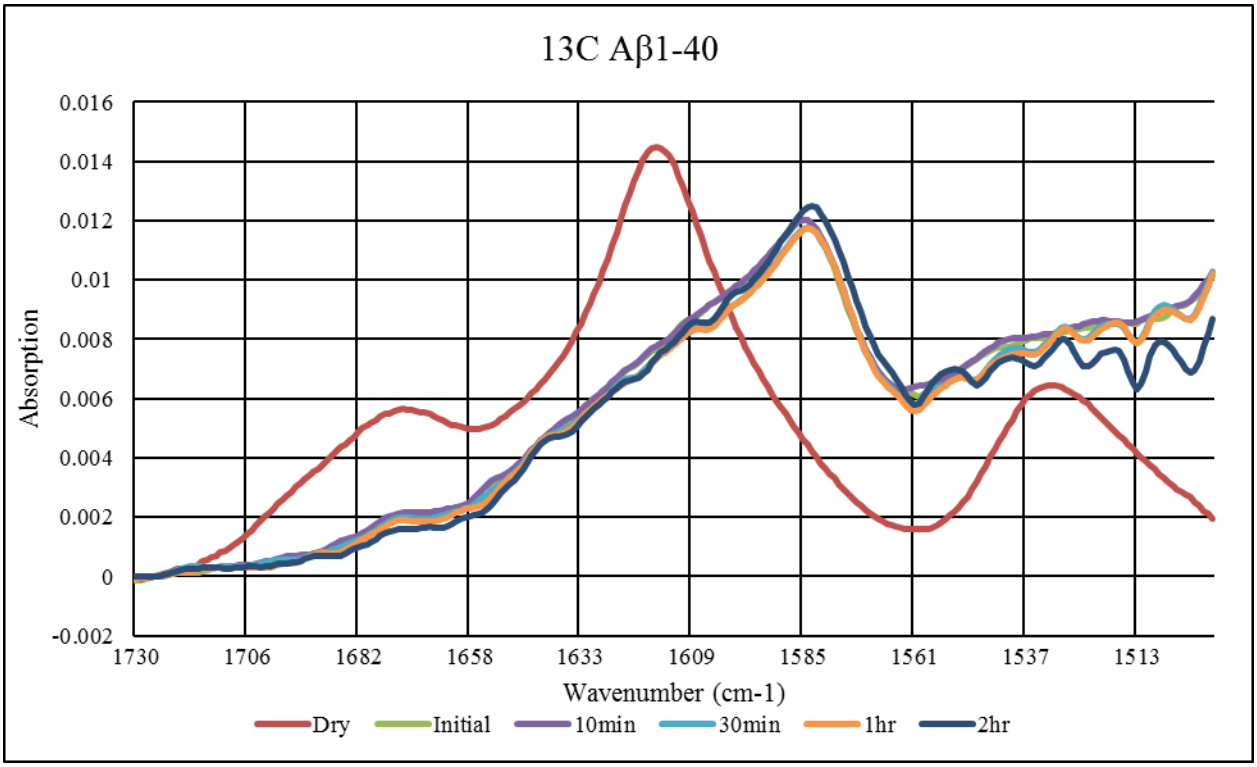

Figure 3

The dry ^{13}C-labeled Aβ$_{1-40}$ peptide shows absorbance signals at 1671 cm^{-1}, 1616 cm^{-1}, and 1530 cm^{-1}. The weak broad signal at 1671 cm^{-1} is assigned to turn structure, the strongest signal at 1616 cm^{-1} corresponds to α-helix structure, and the signal at 1530 cm^{-1} is the amide II signal from the protein backbone. After buffer is added to the sample, there is an almost instant transition to intermolecular β-sheet, shown by an absorption signal at 1583 cm^{-1}, that becomes stronger over the experiment's duration. The turn signal at 1671 cm^{-1} can be seen decreasing over time after addition of buffer. Thus, the initial α-helical and turn structures entirely transition

to β-sheet structure in aqueous buffer. The amide II signal disappears because of amide H/D exchange.

$A\beta_{pE3-40}$

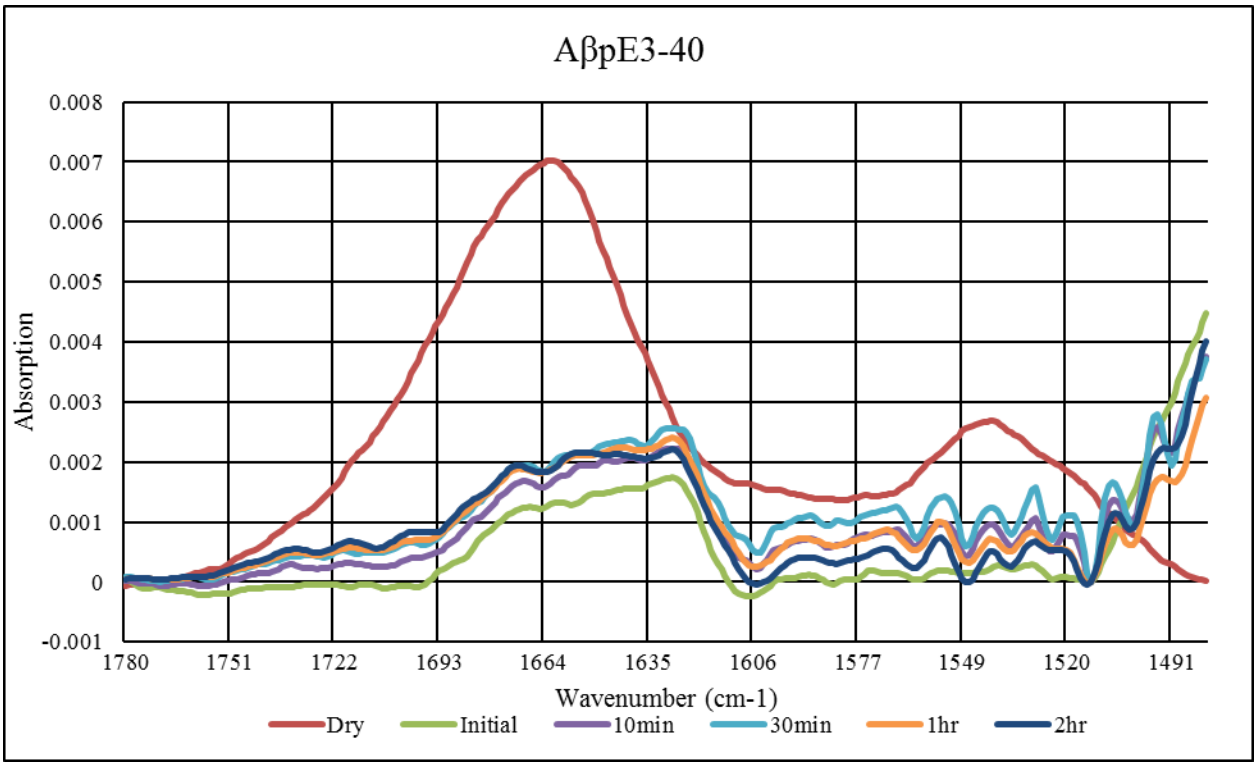

Figure 4

The dry $A\beta_{pE3-40}$ peptide shows a main signal at 1660 cm^{-1}, corresponding to α-helix structure, and an amide II signal at 1539 cm^{-1}. After addition of buffer, the main α-helical peak is replaced by a major feature at 1628 cm^{-1}, assigned to intermolecular β-sheet structure, and a shoulder at 1670 cm^{-1}, indicating a turn structure. The amide II band disappears due to amide H/D exchange.

1:1 Combination of ^{13}C-Labeled A$\beta_{1\text{-}40}$ and Non-Labeled A$\beta_{pE3\text{-}40}$

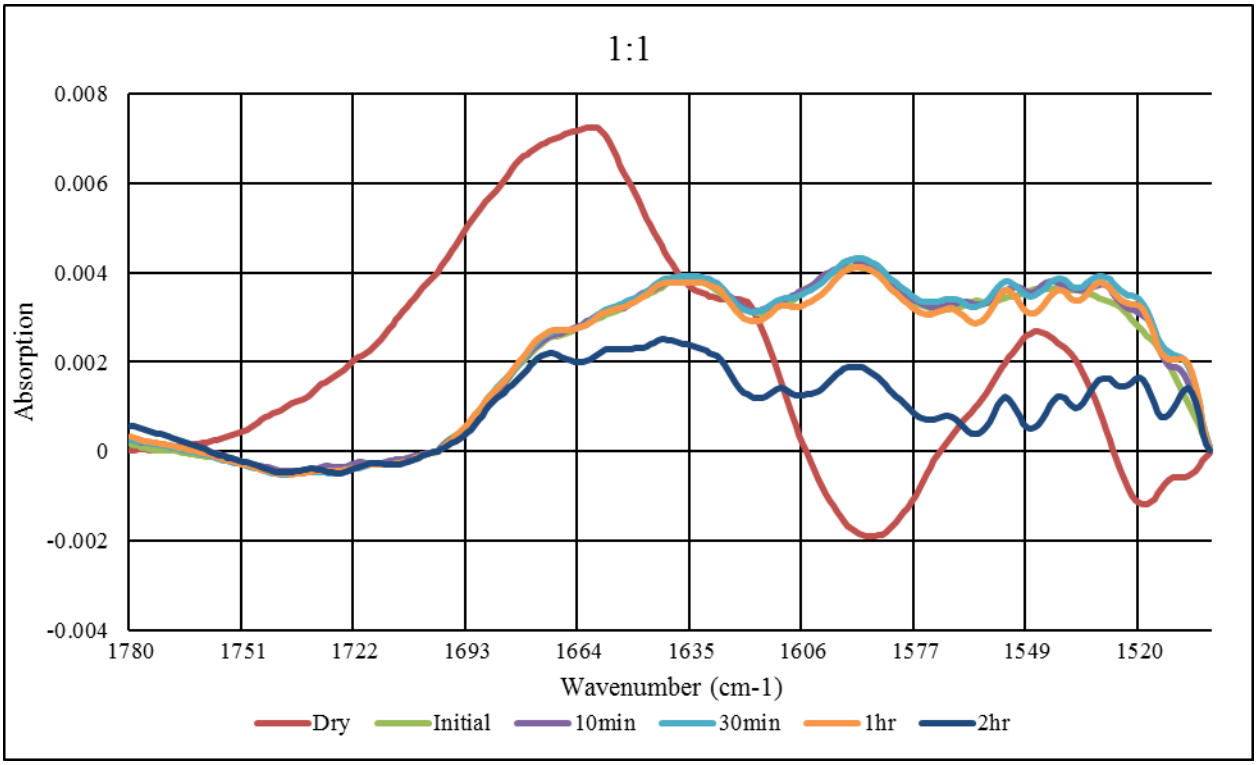

Figure 5

The FTIR spectrum of the dry sample of ^{13}C-labeled A$\beta_{1\text{-}40}$ and non-labeled A$\beta_{pE3\text{-}40}$ combined at 1:1 molar ratio displays amide I band with a major peak around 1658 cm^{-1}, shoulders at 1680 cm^{-1} and 1620 cm^{-1}, and an amide II band at 1544-1535 cm^{-1}. The peaks at 1658 cm^{-1} and 1620 cm^{-1} correspond to α-helical structures of A$\beta_{pE3\text{-}40}$ and ^{13}C-A$\beta_{1\text{-}40}$ peptides, respectively. The ^{13}C-labeled peptide has a smaller extinction coefficient, as detected earlier. The shoulder at 1680 cm^{-1} is assigned to a turn structure. After buffer addition, transition to intramolecular β-sheet structure is observed, manifested by signals around 1635 cm^{-1} and 1592 cm^{-1}, which are generated by the unlabeled A$\beta_{pE3\text{-}40}$ and ^{13}C-labeled A$\beta_{1\text{-}40}$ peptides, respectively. Of note, the β-sheet frequencies in combined peptides are significantly (7-9 cm^{-1}) higher than in

individual peptides. This shift in absorbance signal to a higher wavenumber indicates that when in combination, $A\beta_{1\text{-}40}$ and $A\beta_{pE3\text{-}40}$ form intramolecular β-sheet as opposed to intermolecular β-sheet, when they are separated.

DISCUSSION

The CD spectra show that both peptides assume α-helix conformation while dissolved in HFIP (**Figure 2**). This serves an as important control by providing the initial structure of the peptides before they are dried and then placed in aqueous buffer. In the brain, the Aβ sequence corresponds to the juxtamembrane and the α-helical transmembrane domain of APP. Only when Aβ is proteolytically cleaved does it undergo α-helix to β-sheet structural transition, which underlies peptide aggregation, fibrillogenesis, and toxicity. Elucidation of the structural details of such structural transitions is therefore important for a better understanding of the cytotoxicity of Aβ and the hypertoxicity the pyroglutamylated Aβ.

The FTIR data highlight key differences in fibrillogenesis of $A\beta_{1\text{-}40}$, $A\beta_{pE3\text{-}40}$, and their 1:1 combination. This equimolar combination is biologically relevant because the fraction of pyroglutamylated Aβ in AD brain can reach 50% of total Aβ. The dry peptides maintain the α-helical structure seen in peptides in HFIP solution, and display some turn structure, suggesting the existence of an helix-turn-helix structure (**Figure 3**, **Figure 4**). In their 1:1 combination, the turn structure is displayed s a shoulder 9-10 wavenumbers higher than when separate, indicating structural changes upon the peptides' interaction.

When aqueous buffer is added to $A\beta_{pE3\text{-}40}$ and $A\beta_{1\text{-}40}$ when separated, they quickly undergo transition from α-helix to intermolecular β-sheet structure. Hydrogen bonding in intermolecular β-sheets is stronger than that in intramolecular β-sheets, resulting in weaker C=O bonds in the former case. Consequently, the amide I bands, generated mostly by C=O stretching vibrations, occur at lower frequencies for of intermolecular β-sheets. When the peptides are

combined at an equimolar ratio, instead of transitioning to intermolecular β-sheet, they transition to β-sheets supported by intramolecular hydrogen bonds, shown by absorption at significantly higher wavenumbers (**Figure 5**). These spectral differences indicate inhibition of intermolecular β-sheet formation in the combined peptide sample. This difference is likely to destabilize the process of fibrillogenesis and lead to a greater presence of oligomers, which are known to be far more cytotoxic than fibrils (**Figure 6**). Previous work in this laboratory on structural transitions of $A\beta_{1\text{-}42}$ and $A\beta_{pE3\text{-}42}$ showed similar features, implying that pyroglutamylation increases the cytotoxicity of both 40- and 42-residue Aβ peptides by similar mechanisms, i.e., inhibition of fibrillogenesis and stabilization of oligomeric structures.

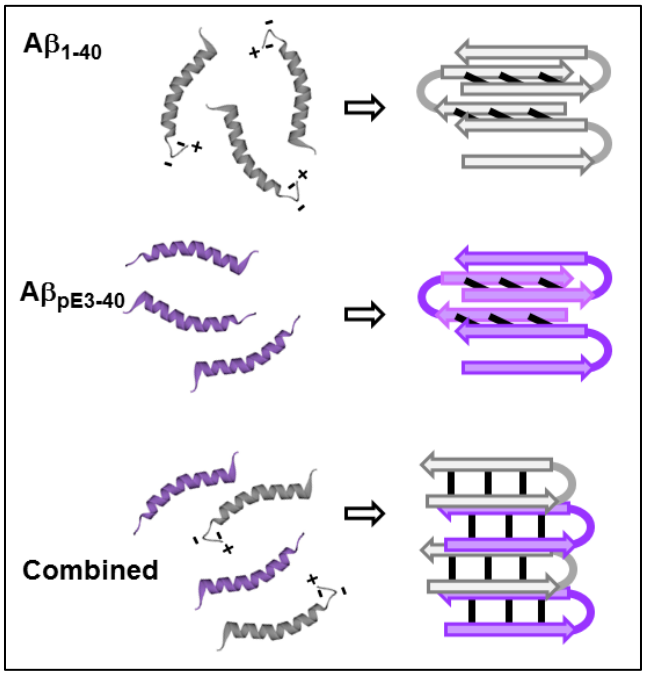

Figure 6

Scheme for aggregation of $A\beta_{1\text{-}40}$ (gray), $A\beta_{pE3\text{-}40}$ (purple), and their combination, accompanied with α-helix to β-sheet transition. At the N-terminus of $A\beta_{1\text{-}40}$ there are 3 additional charges, a positive charge of the N-terminal α -

amino group and 2 negative charges of the side chains of Asp_1 and Glu_3. Helices are shown as spirals, β-strands as arrows, and H-bonds as black bars.

An extension of this study may look at different ratios of $A\beta_{pE3\text{-}40}$ to $A\beta_{1\text{-}40}$, to identify the threshold ratio need to cause inhibition of fibrillogenesis as well as identifying a ratio that produces a maximum inhibition of fibrillogenesis. Once these thresholds are identified, cytotoxicity studies may reveal more precisely how large the difference in cytotoxicity between ratios is. An application of cytotoxic species identification is the development of antibodies against them. Anti-oligomeric antibodies may be used for immunodiagnostics or immunotherapy in AD.

CONCLUSIONS

The primary conclusion drawn from this work is that while both $A\beta_{1\text{-}40}$ and $A\beta_{pE3\text{-}40}$ transition from α-helix to intermolecular β-sheet upon exposure to aqueous buffer when separated, in combination they form β-sheets supported by intramolecular hydrogen bonding. The action of $A\beta_{pE3\text{-}40}$ on $A\beta_{1\text{-}40}$ plausibly leads to inhibition of fibrillogenesis and stabilization of the more toxic oligomers, given that fibrils are supported by intermolecular hydrogen bonding and oligomers are supported by intramolecular hydrogen bonding. This finding is clinically relevant because it implies that peptide mixtures that contain the N-truncated $A\beta_{pE3\text{-}40}$ also form more stable oligomers and hence are more toxic. Given that it is Aβ oligomers that are the major cytotoxic entity in AD, our data offer strategies for identifying new AD biomarkers that can be targeted for development of novel diagnostic and immunotherapeutic approaches.

REFERENCES

Agostinho, P., Pliassova, A., C.R., O., & R.A., C. (2015). Localization and Trafficking of Amyloid β Protein Precursor and Secretases: Impact on Alzheimer's Disease. *J Alzheimers Dis, 45*(2), 329-47.

Ankarcrona, M., Winblad, B., Monteiro, C., Fearns, C., Powers, E., Johansson, J., . . . Kelly, J. (2016). Current and Future Treatment of Amyloid Diseases. *Journal of Internal Medicine, 280*(2), 177-202.

Awasthi, M., Singh, S., Pandey, V. P., & Dwivedi, U. N. (2016). Alzheimer's disease: An overview of amyloid beta dependent pathogenesis and its therapeutic implications along with in silico approaches emphasizing the role of natural products. *Journal Of The Neurological Sciences, 361*(1878-5883), 256.

Barage, S. H., & Sonawane, K. D. (2015). Amyloid cascade hypothesis: Pathogenesis and therapeutic strategies in Alzheimer's disease. *Neuropeptides, 52*(1532-2785), 1-18.

Bayer, T., & Wirths, O. (2014). Focusing the amyloid cascade hypothesis on N-truncated Abeta peptides as drug targets against Alzheimer's disease. *ACTA NEUROPATHOLOGICA, 127*(6), 787-801.

Beel, A., & Sanders, C. (2008). Substrate Specificity of γ-Secretase and Other Intramembrane Proteases. *Cell Mol Life Sci, 65*(9), 1311-1334.

Bird, T. (2015). Alzheimer's Disease Overview. (R. Pagon, M. Adam, H. Ardinger, & e. al., Eds.) Seatle, Washington, USA.

Cipriani, G., Dolciotti, C., Picchi, L., & Bonuccelli, U. (2011). Alzheimer and his disease: a brief history. *Neurological Sciences, 32*(2), 275-279.

Dickson, D. (2004). Apoptotic Mechanisms in Alzheimer Neurofibrillary Degeneration: Cause Or Effect? *The Journal of Clinical Investigation, 114*(1), 23-27.

Ehret, M. J., & Chamberlin, K. W. (2015). New Drug Review: Current Practices in the Treatment of Alzheimer Disease: Where is the Evidence After the Phase III Trials? *In Clinical Therapeutics, 37*(8), 1604-1616.

Goedert, M. (2015). Alzheimer’s and Parkinson’s diseases: The prion concept in relation to assembled Aβ, tau, and α-synuclein. *Science, 349*(6248), 1-9.

Goldblatt, G., Matos, J., Gornto, J., & Tatulian, S. (2015). Isotope-edited FTIR reveals distinct aggregation and structural behaviors of unmodified and pyroglutamylated amyloid β peptides. *Physical Chemistry Chemical Physics, 17*(48), 32149-32160.

Gralle, M., & Ferreira, S. T. (2007). Structure and Functions of the Human Amyloid Precursor Protein: The Whole is More Than the Sum of its Parts. *Progress in Neurobiology, 82*(1), 11-32.

Herrmann, N., Chau, S. A., Kircanski, I., & Lanctot, K. L. (2011). Current and Emerging Drug Treatment Options for Alzheimer's Disease: A Systematic Review. *Drugs, 17*(15), 2031-2065.

Hetson, L. (1977). Alzheimer's Disease, Trisomy 21, and Myeloproliferative Disorders. *Science, 196*(4287), 322-323.

Holtzman, D. (2011). Alzheimer's Disease: The Challenge of the Second Century. *Science Translational Medicine, 3*(77), 17.

Jayne, T. N., Verdile, G., Sutherland, G., Münch, G., Musgrave, I., Moussavi, S., & Lardelli, M. (2016). Evidence For and Against a Pathogenic Role of Reduced γ-Secretase Activity in Familial Alzheimer's Disease. *Journal Of Alzheimer's Disease, 52*(3), 781-799.

Klevanski, M., Herrmann, U., Weyer, S. W., Fol, R., Cartier, N., Wolfer, D. P., . . . Muller, U. C. (2015). The APP Intracellular Domain is Required for Normal Synaptic Morphology, Synaptic Plasticity, and Hippocamus-Dependent Behavior. *Neurobiology of Disease, 35*(49), 16018-16033.

Lim, Y., Villemagne, V., Pietrzak, R., Ames, D., Ellis, K. A., Harrington, K., . . . Maruff, P. (2015). APOE ε4 moderates amyloid-related memory decline in preclinical Alzheimer's Disease. *Neurobiology Of Aging, 36*(3), 1239-1244.

Lin, Y., Wang, J., Wang, K., Liao, J., & Cheng, I. H. (2014). Differential regulation of amyloid precursor protein sorting with pathological mutations results in a distinct effect on amyloid-β production. *Journal Of Neurochemistry, 131*(4), 407-412.

Mandler, M., Walker, L., Santic, R., Hanson, P., Upadhaya, A., Colloby, S., . . . Attems, J. (2014). Pyroglutamylated amyloid-beta is associated with hyperphosphorylated tau and severity of Alzheimer's disease. *ACTA NEUROPATHOLOGICA, 128*(1), 67-79.

Miles, A., & Wallace, B. (2016). Circular Dichroism Spectroscopy of Membrane Proteins. *Chemical Society Reviews, 45*(18), 4859-4872.

Miller, D., Currie, J., Iqbal, K., Potempska, A., & Styles, J. (1989). Relationships Among The Cerebral Amyloid Peptides And Their Precursors. *Informa Healthcare, 21*(2), 83-87.

Mohamed, T., Shakeri, A., & Rao, P. P. (2016). Amyloid cascade in Alzheimer's disease: Recent advances in medicinal chemistry. *European Journal of Medicinal Chemistry, 113*(1768-3254), 258-272.

O'Brien, R., & PC, W. (2011). Amyloid Precursor Protein Processing and Alzheimer's Disease. *Annu Rev Neurosci, 34*(1545-4126), 185-204.

Paravastu, A. K., Leapman, R. D., Yau, W.-M., & Tycko, R. (2008). Molecular structural basis for polymorphism in Alzheimer's β-amyloid fibrils. *PNAS, 105*(47), 18349-18354.

Qiang, W., Yau, W.-M., Lu, J.-X., Collinge, J., & Tycko, R. (2017). Structural variation in amyloid-β fibrils from Alzheimer's disease clinical subtypes. *Nature, 541*(7636), 217-221.

Schilling, S., Kohlmann, S., Bauscher, C., Sedlmeier, R., Koch, B., Eichentopf, R., . . . Demuth, H. (2011). Glutaminyl Cyclase Knock-out Mice Exhibit Slight Hypothyroidism but No Hypogonadism. *JOURNAL OF BIOLOGICAL CHEMISTRY, 286*(16), 14199-14208.

Sofronescu, A. G. (2015, August 10). *Cerebrospinal Fluid Analysis*. Retrieved from Medscape: www.emedicine.medscape.com/article/2093316-overview

Takei, H., Kosarac, O., & Powell, S. (2009). Cytomorphologic Manifestations of Alzheimer's Disease Using Brain Squash Smears: An Autopsy Study With Histology-Cytology Correlation. *Diagnostic Cytopathology, 37*(9), 654-660.

Tycko, R. (2016). Alzheimer's Disease: Structure of Aggregates Revealed. *Nature*, *537*(7621), 492.